Highly Precised and Efficient Robot-Based ESPAR Antenna Measurements in Realistic Environments

Mateusz Groth[1], Kamil Domanski[2], Krzysztof Nyka[3], Lukasz Kulas[4]
Department of Microwave and Antenna Engineering,
Faculty of Electronics, Telecommunications and Informatics, Gdansk University of Technology 80-233 Gdansk, Poland,
[1]mateusz.groth@pg.edu.pl, [2]kamil.domanski@pg.edu.pl, 3krzysztof.nyka@pg.edu.pl, [4]lukasz.kulas@pg.edu.pl

***Abstract*— In this paper, we present a novel approach utilizing a small Unmanned Surface Vehicle (USV) equipped with Global Navigation Satellite System (GNSS) technology to facilitate large-scale outdoor automated measurements. The system employs dedicated software and measurement scripts to autonomously navigate the robot along predefined routes, stopping at multiple points for data collection. This method minimizes observational error and enables the efficient verification and validation of DoA and positioning algorithms. We provide a detailed overview of the robot's architecture, operating modes, and system performance, demonstrating its capability to achieve high accuracy and repeatability in measurements. Additionally, we present results from a DoA estimation experiment using an electronically steerable parasitic array radiator (ESPAR) antenna, showcasing the system's ability to provide precise and consistent measurements across various transmission module heights.**

***Index Terms*— antenna measurements, robotic measurements, direction-of-arrival (DoA), ESPAR antenna, internet-of-things (IoT), wireless sensor networks (WSN).**

I. INTRODUCTION

With the development of technology, robots and autonomous vehicles become more and more popular for performing repetitive tasks that require high-precision operations, not only in high-cost manufacturing, such as car factories, but also in relatively simple applications. Continuous increase of accessible computational power and mechanical components allows to utilize Unmanned Aerial Vehicles (UAVs) and Unmanned Ground Vehicles (UGVs) in many applications, ranging from safety and security applications such as wildfires [1], production [2], or healthcare [3], becoming a part of day-to-day tasks. Utilizing robots increases productivity, efficiency and, in most applications, accuracy of realized tasks [4].

Another wide range of applications for robots and autonomous vehicles is to perform measurements for calibration and validation of other systems, such as wireless positioning. To calibrate a fingerprint-based indoor positioning system a radio map of the area, being a spatial distribution of the received signal strength, is necessary [5]. Most often the radio map is created by a human operator who performs the measurements in the area. There are solutions that additionally utilize various approaches such as reference nodes [6] or mathematical processing, such as interpolation or regression, to increase the density of the map or reduce time and work effort [7]. Despite these enhancements, it is still crucial to periodically update the map to maintain accuracy over time [8].

Furthermore, for validation and verification of many newly developed position estimation methods, such as Direction of Arrival (DoA) or RF-based localization, measurements in certain known points have to be performed so that the position estimation can be then verified with accurate data in relevant testing environments. It is important that the measurements are precise and repetitive, with the aim of minimizing the human error factor in the total estimation error. The main challenge in such tasks is that the measurements are often time-consuming, especially when performed in large areas or with high density of testing points. This may also introduce risks of human error leading to the loss of the measurement precision or quality over time. Nowadays, there are techniques to automate such measurements, e.g. by using a turntable [9], however, these are usable only for rotary measurements for angular scanning and, due to the dimensions and weight of the device, in most cases, they are limited to a single room (i.e., anechoic chamber) in which they are installed.

In this paper, we propose a technique that utilizes a small USV to facilitate large-area and outdoor automated measurements of radio signals. The robot is equipped with a GNSS module and positioning system to determine its position with 1 cm accuracy Dedicated software, integrated with the measurement scripts, allows to autonomously move the device-under-test (whose position is being estimated) in a predefined manner, following the predefined route and stopping for data collection. Additionally, depending on the measurement scenario, the robot can stop at multiple points as well as move to the exact same location repeatedly. As a result, the observational error of the measurement is minimized. To the best authors' knowledge, no similar setup for verification and validation of DoA and RF-based positioning algorithms, especially maintaining the robot's self-localization accuracy within 1 cm in all three axes, has been reported in available literature.

II. SYSTEM ARCHITECTURE

A. Robot overview

The testing robot is a four-wheel-drive, skid-steer, and highly flexible mobile testing platform capable of executing preplanned routes with self-localization accuracy up to 1 cm.

Figure 1: Robot for automated outdoor measurements

The robot's dimensions are 44 cm x 50 cm x 28 cm, and its low weight, up to 17 kg, facilitates easy transportation and deployment in the field. Thanks to its inflatable tires and powerful drive system, the robot can operate seamlessly on uneven terrain, such as large lawn areas or unpaved roads.

One of the significant advantages of the robot is its extended operating time, which can reach up to 8 hours when performing the measurements described in this paper. The robot can operate in two modes:

1. Remote Control Mode: In this mode, the operator has full control over the robot's movement using a remote radio controller.
2. Autonomous Waypoint Mission: In this mode, the operator can either preplan the entire mission or send goals one by one. In the former case, the robot follows a predefined route consisting of a list of waypoints where it conducts measurements. In the latter case, waypoints are transmitted to the robot one by one via the MQTT protocol. Upon receiving a waypoint, the robot promptly initiates movement toward the specified destination. After reaching each designated waypoint, the robot comes to a halt, performs measurements, and awaits further instructions.

B. Robot Architecture

The primary component of the robot is a single-board computer (SBC) equipped with an Intel Core i7 processor, which offers substantial computing power for this specific use case. The SBC is responsible for supervising the robot's movement performance and its software receives commands via MQTT from the measurement supervision software, which handles all aspects of measurements.

In autonomous waypoint mission mode, the route is typically preloaded into the software, allowing the computer to await the 'move to the next point' command. Once the command is received, the main computer transmits the required destination to the autopilot. After reaching the desired destination, the SBC sends precise localization information to the supervision software, initiating the measurement process.

Another critical component of the robot is the autopilot, responsible for controlling the robot's movement. Information regarding the robot's position and orientation is provided by two high-precision GNSS receivers utilizing real time kinematic (RTK) technology and a dedicated software. This technology enables the autopilot to control the motors effectively to achieve the desired location.

To maintain 1 cm positioning accuracy, the positioning algorithm analyses current rotation and pitch deviation considering this data for the position determination.

Throughout the measurement process, the operator can assume control of the robot using an RC remote radio at any moment. This feature offers both convenience and an additional layer of safety.

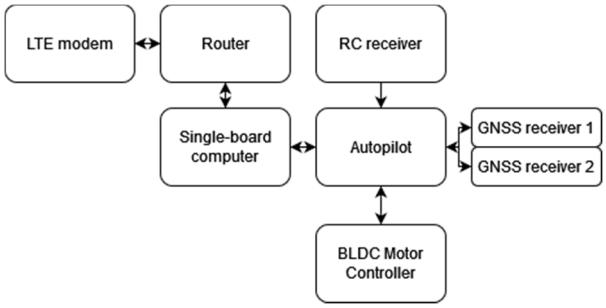

Figure 2: Robot hardware architecture

III. SYSTEM PERFORMANCE

An illustration of the standard measurement setup is presented in Figure 3. In this figure, the blue line represents the planned route, the green points indicate the measurement locations, and the red line traces the actual trajectory of the robot. Due to imperfect tuning of control algorithms, the actual trajectory of the robot may deviate from the planned path. The cross-track error of the robot's path execution is depicted in Figure 4.

Figure 3: Example of a Measurement Mission.

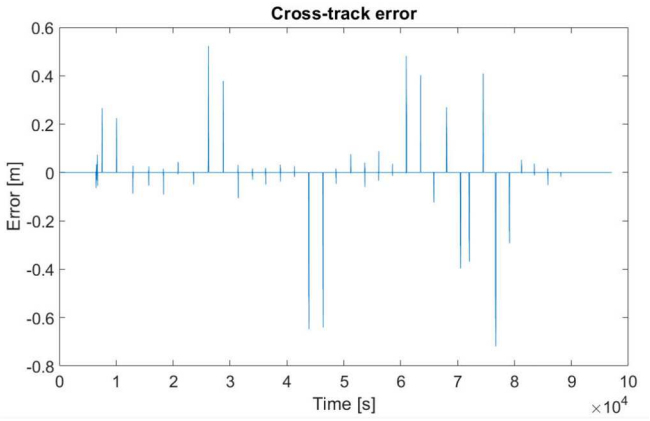

Figure 4: Cross-track error of the robot's path execution.

In the worst-case scenario, the robots deviate by approximately 0.7 meters from the planned path while standard deviation is 0.036 meter. However, in the specific use case presented in this paper, the precision of self-localization of the robot at the measurement spots is of greater importance than the accuracy of tracking the planned route. This prioritization stems from the crucial nature of knowing the precise measurement location, even if it does not precisely match the initial plan.

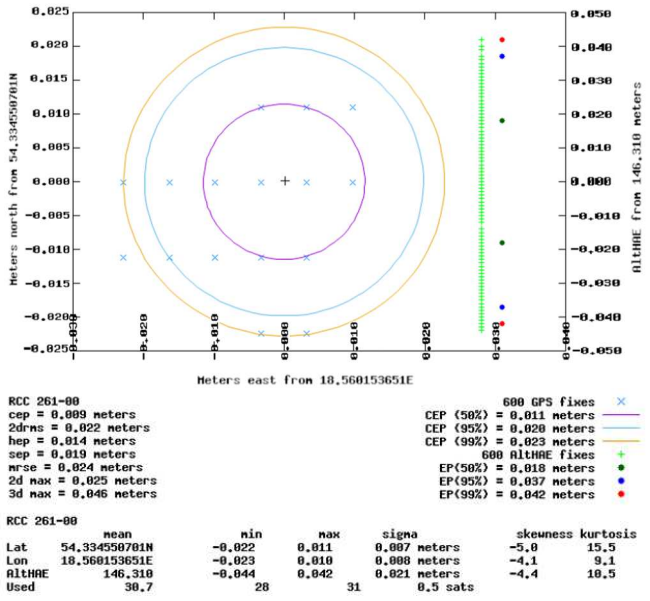

Figure 5: Localization accuracy measurements.

The results of the localization accuracy measurements, encompassing 600 sample points are presented in Figure 5. It reveals that 99% of the position fixes fall within a 2.3-cm diameter, with standard deviations in the lateral and longitudinal directions of 0.7 cm and 0.8 cm, respectively. The achieved accuracy is more than sufficient to evaluate the performance of the RF-based positioning and DoA estimation systems. The convenience of repeatability of measurements and ease of deployment significantly surpasses the standard measurement methods employed thus far.

IV. Robot-based DoA Measurements

A. Measurement setup

To verify the robot-based measurement setup, we prepared an outdoor testbed for DoA estimation, similar to the one described in [10], where measurements were done manually. The setup consists of an electronically steerable parasitic array radiator (ESPAR) antenna, placed in the center of 10 meters diameter circle. The antenna has been connected to a dedicated Bluetooth Low Energy nRF52840-based module.

Figure 6: ESPAR antenna used in measurements

The antenna has been installed facing down on a tripod at the height of 258 cm. A dedicated 3D printed mounting system has been designed that allows to eliminate the potential influence of metal elements in the antenna surroundings. For transmitters, four Bluetooth Low Energy Nordic nRF52840 dongles with integrated microstrip antenna has been used, installed on the robot at 3 different heights. Each module has been set to broadcast BLE advertising packets with different transmission power, as presented in Table 1. The aim of the measurement was to test the accuracy of the estimation using the setup with active and passive elements of ESPAR antenna oriented towards the ground and with transmitters located on heights different than the ESPAR antenna, so that the vertical angle $\theta \neq 90^\circ$.

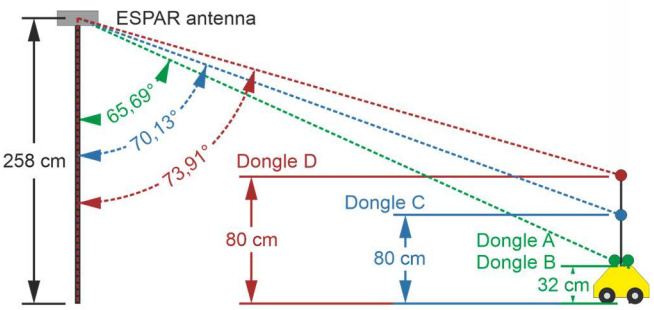

Figure 7: Transmitter and ESPAR antenna setup - side view

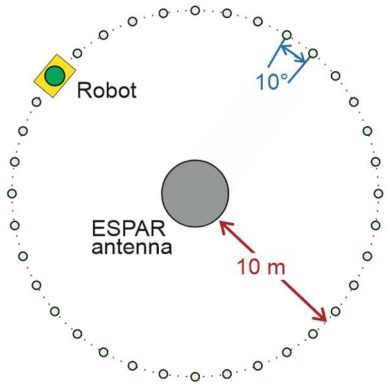

b

Figure 8: Transmitter and ESPAR antenna setup top view

TABLE 1: TRANSMITTER SETUP

Dongle	Height [cm]	Transmission power [dBm]	Vertical angle θ
A	32	-12	65.69°
B	32	8	65.69°
C	80	0	70.13°
D	115	8	73.91°

For the measurement, a mission for a robot was programmed to follow the edge of the circle and stop every $\Delta\varphi = 10^{\circ}$ to initiate the data transmission of 100 packets at each of three available broadcast channels. The transceiver with ESPAR antenna measured received signal strength (RSS) for 12 directional antenna radiation patterns, as described in [10]. Once the transmission is done, the robot moved to the next position. Collected data was tramsitted via dedicated Wi-Fi network to the PC and stored using MQTT data storage.

a b

Figure 9: Test setup components. a) robot with nRF52 dongles installed, b) ESPAR antenna in 3D printed housing

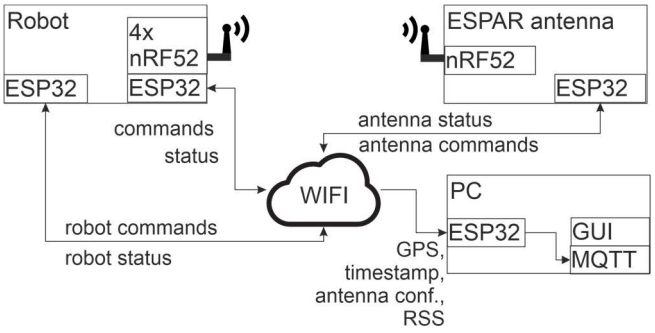

Figure 10: Measurement setup architecture

B. *Results*

Collected values were used as an input data for Power Pattern Cross Correlation (PPCC) [11] algorithm, using ESPAR antenna radiation patterns measured in anechoic chamber for $\theta = 60^{\circ}$. Based on the measured RSS data, DoA estimation was performed. Cumulative DoA estimation results based on the PPCC algorithm are shown in Table 2.

TABLE 2: DOA ACCURACY CUMULATED RESULTS

Channel	Dongle	Precision	RMSE
37	A	13°	6.14°
	B	14°	7.08°
	C	13°	4.50°
	D	11°	4.87°
38	A	12°	5.12°
	B	12°	6.83°
	C	17°	6.99°
	D	13°	5.00°
39	A	16°	6.72°
	B	23°	8.59°
	C	25°	10.37°
	D	11°	4.73°

It can be easily noticed, that the system provides similar results for each tested height of transmission module, even despite deviation $\Delta\theta = 13.91^{\circ}$ for module located at the height of 115 cm. Estimation error for each of 36 test points and four transmitting sources is presented on Figure 4. Full autonomous measurement process for the setup of 36 measurement points has taken 93 minutes. During the measurements, no operator involvement was needed.

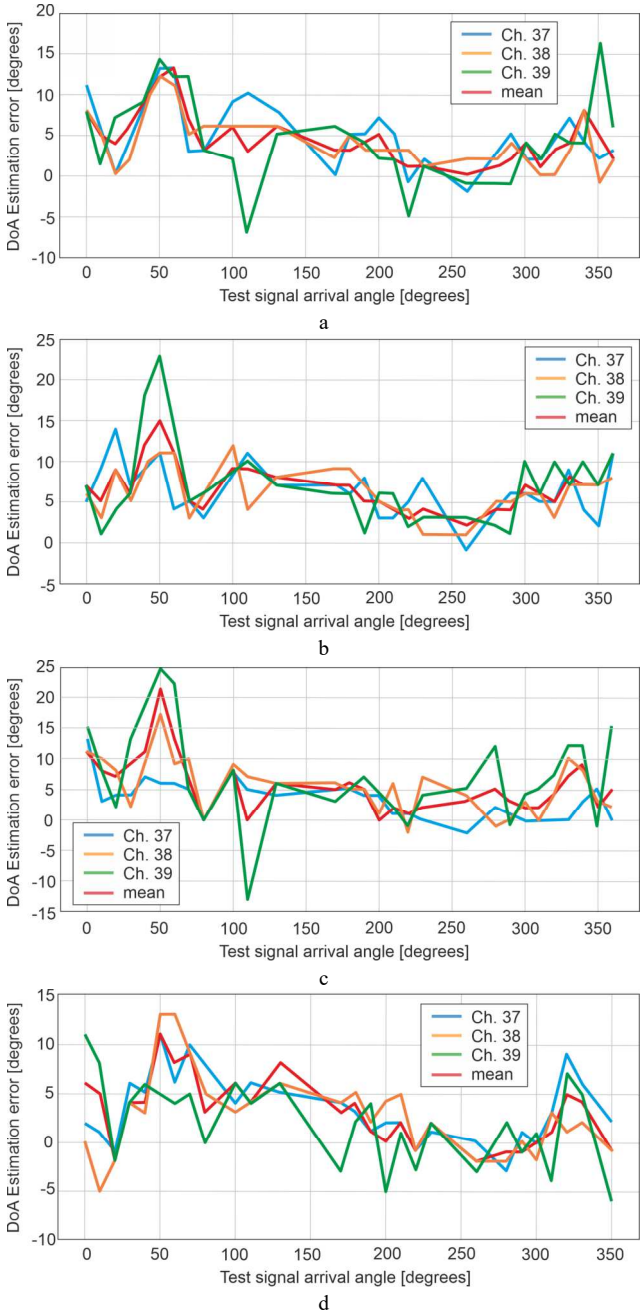

Figure 11: DoA estimation errors obtained from the measurements for: a) module A, b) module B, c) module C, d) module D

V. Conclusions

This paper introduces an innovative and practical solution to address the challenges of precise and repetitive measurements for the calibration and validation of positioning and DoA estimation systems. The conventional methods, which often require human involvement, are susceptible to errors and can be time-consuming, particularly for large-scale measurements.

The proposed approach leverages a small USV equipped with advanced GNSS technology. The USV is capable of autonomously executing predefined routes and stopping at multiple locations for data collection. The GNSS module ensures accurate self-localization within 1 cm, substantially reducing observational errors in the measurement process.

The results show that the system is capable of performing autonomous measurements providing algorithms and methods validation in an efficient manner. Moreover, the autonomous measurement process significantly reduces the time required for measurement, and the absence of operator involvement during measurements enhances convenience and efficiency.

Acknowledgment

This work has been supported by project TRANSACT, funded from the KDT Joint Undertaking (JU) under grant agreement No 101007260. The JU receives support from the European Union's Horizon 2020 research and innovation programme and Netherlands, Finland, Germany, Poland, Austria, Spain, Belgium. Denmark, Norway.

References

[1] M. A. Akhloufi, A. Couturier, and N. A. Castro, "Unmanned Aerial Vehicles for Wildland Fires: Sensing, Perception, Cooperation and Assistance," *Drones*, vol. 5, no. 1, p. 15, Feb. 2021, doi: 10.3390/drones5010015.

[2] Ş. Çiğdem, I. Meidute-Kavaliauskiene, and B. Yıldız, "Industry 4.0 and Industrial Robots: A Study from the Perspective of Manufacturing Company Employees," *Logistics*, vol. 7, no. 1, p. 17, Mar. 2023, doi: 10.3390/logistics7010017.

[3] A. A. Morgan, J. Abdi, M. A. Q. Syed, G. E. Kohen, P. Barlow, and M. P. Vizcaychipi, "Robots in Healthcare: a Scoping Review," *Curr. Robot. Rep.*, vol. 3, no. 4, pp. 271–280, Oct. 2022, doi: 10.1007/s43154-022-00095-4.

[4] P. Barosz, G. Gołda, and A. Kampa, "Efficiency Analysis of Manufacturing Line with Industrial Robots and Human Operators," *Appl. Sci.*, vol. 10, no. 8, p. 2862, Apr. 2020, doi: 10.3390/app10082862.

[5] K. Kaemarungsi and P. Krishnamurthy, "Properties of indoor received signal strength for WLAN location fingerprinting," in *The First Annual International Conference on Mobile and Ubiquitous Systems: Networking and Services, 2004. MOBIQUITOUS 2004.*, Boston, MA, USA: IEEE, 2004, pp. 14–23. doi: 10.1109/MOBIQ.2004.1331706.

[6] A. T. Le *et al.*, "Unbalanced Hybrid AOA/RSSI Localization for Simplified Wireless Sensor Networks," *Sensors*, vol. 20, no. 14, p. 3838, Jul. 2020, doi: 10.3390/s20143838.

[7] D. J. Suroso, F. Y. M. Adiyatma, P. Cherntanomwong, and P. Sooraksa, "Fingerprint Database Enhancement by Applying Interpolation and Regression Techniques for IoT-based Indoor Localization," *Emerg. Sci. J.*, vol. 4, pp. 167–189, Jan. 2022, doi: 10.28991/esj-2021-SP1-012.

[8] A. S. Yaro, F. Maly, and P. Prazak, "A Survey of the Performance-Limiting Factors of a 2-Dimensional RSS Fingerprinting-Based Indoor Wireless Localization System," *Sensors*, vol. 23, no. 5, p. 2545, Feb. 2023, doi: 10.3390/s23052545.

[9] M. Plotka, M. Tarkowski, K. Nyka, and L. Kulas, "A novel calibration method for RSS-based DoA estimation using ESPAR antennas," in *2018 22nd International Microwave and Radar Conference (MIKON)*, Poznan, Poland: IEEE, May 2018, pp. 65–68. doi: 10.23919/MIKON.2018.8405316.

[10] M. Groth, M. Rzymowski, K. Nyka, and L. Kulas, "ESPAR Antenna-Based WSN Node With DoA Estimation Capability," *IEEE Access*, vol. 8, pp. 91435–91447, 2020, doi: 10.1109/ACCESS.2020.2994364.

[11] E. Taillefer, A. Hirata, and T. Ohira, "Direction-of-arrival estimation using radiation power pattern with an ESPAR antenna," *IEEE Trans. Antennas Propag.*, vol. 53, no. 2, pp. 678–684, Feb. 2005, doi: 10.1109/TAP.2004.841312.